Electronic Supplementary Information 1

1. Sample preparation

$Ce_2Zr_2O_8$ prepared by co-precipitation of aqueous solutions of $Ce(NO_3)_3 \cdot 6H_2O$ and $ZrO(NO_3)_2 \cdot 2H_2O$ [6] (obtained from Toyota Central R&D Labs. Inc.), was calcined at 773 K for 3 h. $Ni(NO_3)_2 \cdot 6H_2O$ (Ni 1 wt%) was impregnated to the calcined $Ce_2Zr_2O_8$ in water, and the obtained sample was dried, followed by calcination at 773 K for 3 h ($NiO_x/Ce_2Zr_2O_8$). 10 mg of prepared $NiO_x/Ce_2Zr_2O_8$ were suspended into 100 ml of ethanol with ultra-sonic vibration. Then a SiO_2 thin membrane (obtained from Atok; 5 mm x 10 mm x 30 μm) was dipped to the suspension and dried in air. These processes were repeated three times and the obtained sample was finally calcined at 773 K for 1 h. A reduced sample ($NiO_x/Ce_2Zr_2O_7$) was prepared by the further treatment of prepared $NiO_x/Ce_2Zr_2O_8$ on the SiO_2 membrane with H_2 (13.3 kPa) at 773 K for 0.5 h. All prepared samples were stored under N_2 atmosphere.

2. XRD

XRD of the oxidized and reduced samples was recorded on a Rigaku Multiflex-STe diffractomator.

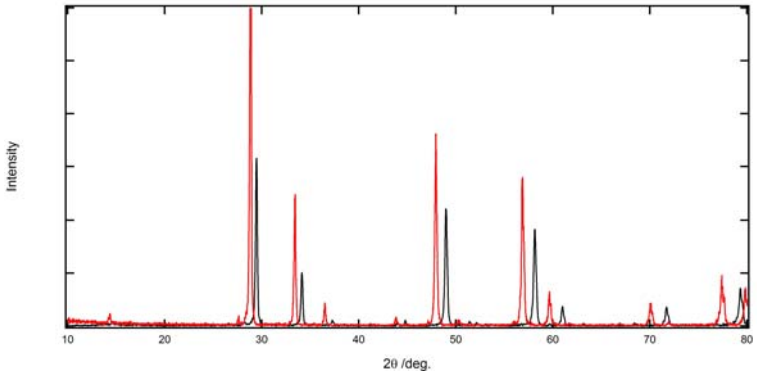

Figure SI 1: XRD patterns of $NiO_x/Ce_2Zr_2O_7$ (red) and $NiO_x/Ce_2Zr_2O_8$ (black).

3. SEM

SEM images of $NiO_x/Ce_2Zr_2O_y$ on SiO_2 membranes were recorded by JEOL JSM-6701F Field Emission SEM in SEI (Secondary Electron Imaging) mode. Electron accelerating volt was 1.0 kV. The average particle size of $NiO_x/Ce_2Zr_2O_y$ and the number of $NiO_x/Ce_2Zr_2O_y$ particles on SiO_2 membranes were estimated by using SEM images (size: 128.0 μm x 102.4 μm). The fractions of isolated and aggregated catalyst particles on the SiO_2 membranes were estimated from the SEM images.

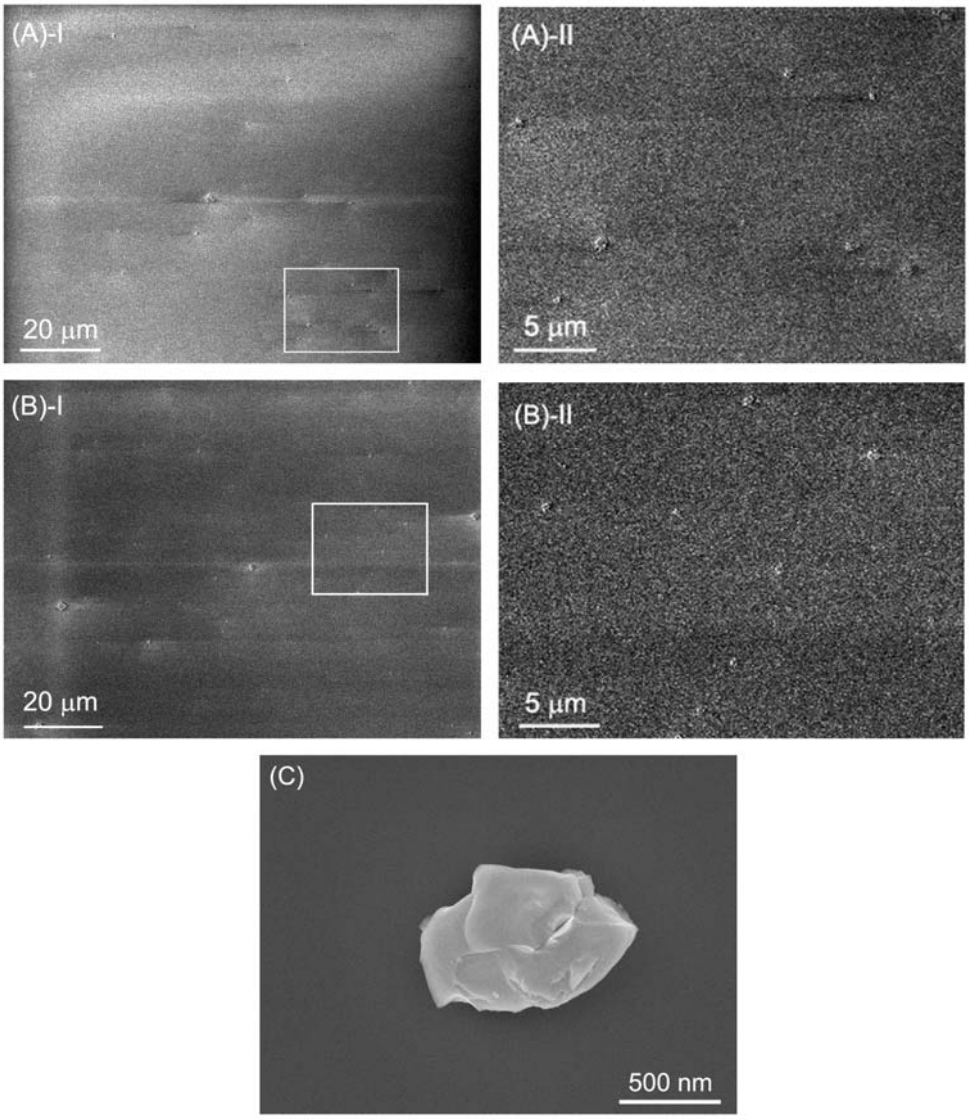

Figure SI 2: SEM images of (A) reduced $NiO_x/Ce_2Zr_2O_7$ and (B) oxidized $NiO_x/Ce_2Zr_2O_8$ dispersed on SiO_2 membranes. White squares in I represent each areas of II. (C) A SEM image of a single particle of $NiO_x/Ce_2Zr_2O_8$ on a Si substrate. The single particle was composed of multi-domains.

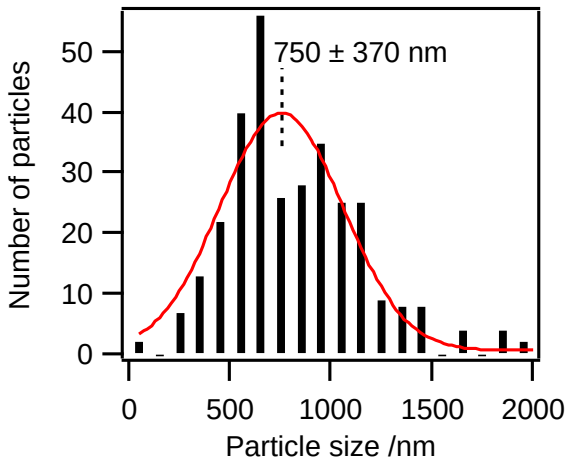

Figure SI 3: Particle size distribution of $NiO_x/Ce_2Zr_2O_y$. Average particle size was estimated to be 750±370 nm.

Table SI 1: Numbers of isolated and aggregated $NiO_x/Ce_2Zr_2O_y$ particles on SiO_2 membranes

Sample	Number of isolated particles	Number of aggregated particles	Density of isolated particles	Aggregated particles %
(A) reduced $NiO_x/Ce_2Zr_2O_7$	52	1	4.0×10^{-3} μm^{-2}	1.9%
(B) oxidized $NiO_x/Ce_2Zr_2O_8$	151	1	1.2×10^{-2} μm^{-2}	0.7%

A SEM image: 128.0 μm x 102.4 μm. The numbers of isolated and aggregated $NiO_x/Ce_2Zr_2O_y$ particles were counted by Figure SI 2 (A)-I or (B)-I, respectively.

(Density of isolated particles) = (number of isolated particles) / (SEM image area of I (128.0 μm x 102.4 μm)).

(Percentage of aggregated particles) = {(number of aggregated particles) / [(number of isolated particles) + (number of aggregated particles)]} x 100.

Electronic Supplementary Information 2

1. μ-XRF and μ-XAFS

Scanning μ-XRF and μ-XAFS measurements were conducted at the BL37XU undulator beamline at SPring-8 (8 GeV, 100 mA). X-rays from an undulator were monochromatized by a Si(111) double-crystal monochromator and horizontally and vertically focused by Kirkpatrick-Baez (KB) mirrors (Figure SI 4). The focusing size of the X-ray μ-beam was 1000 nm (h) x 800 nm (v) at Ni K-edge (8332 eV) (Figure SI 5). A SiO_2 membrane dispersing the Ni catalyst particles was enclosed in an in-situ XAFS cell (Figure SI 6) with flowing of N_2. The XAFS cell was mounted on a piezoelectric translation stage (Physik Instrumente P-517) and the sample was put on the focusing point of the KB mirror.

Fluorescent X-rays emitted from a sample were detected by a 19-element Ge detector. Scanning μ-XRF mapping was performed by X-ray excitation at 8424 eV and the piezoelectric translation stage was moved every 200 nm. 2-Dimensional XRF images were obtained for both Ni Kα (7478 eV) line and Ce Lα (4840 eV) + $L\beta_1$ (5262 eV) lines detected for 1 or 2 s at each point. 2D mapping in Fig. 1 (A) and (B)/(C) was performed for 23 min (2 s x 676 points (26 points (h) x 26 points (v))) and 8 min (1 s x 441 points (21 points (h) x 21 points (v))), respectively. Ni K-edge μ-XANES (150 points) was measured for 45 min at the centre position of high intensity area of the XRF 2D-mapping. The amount of Ni atoms was estimated to be in the order of 10^7 in a catalyst particle of 750 nm in diameter. Ni K-edge μ-EXAFS (300 points) was measured for 3 h at a similar position to the μ-XANES.

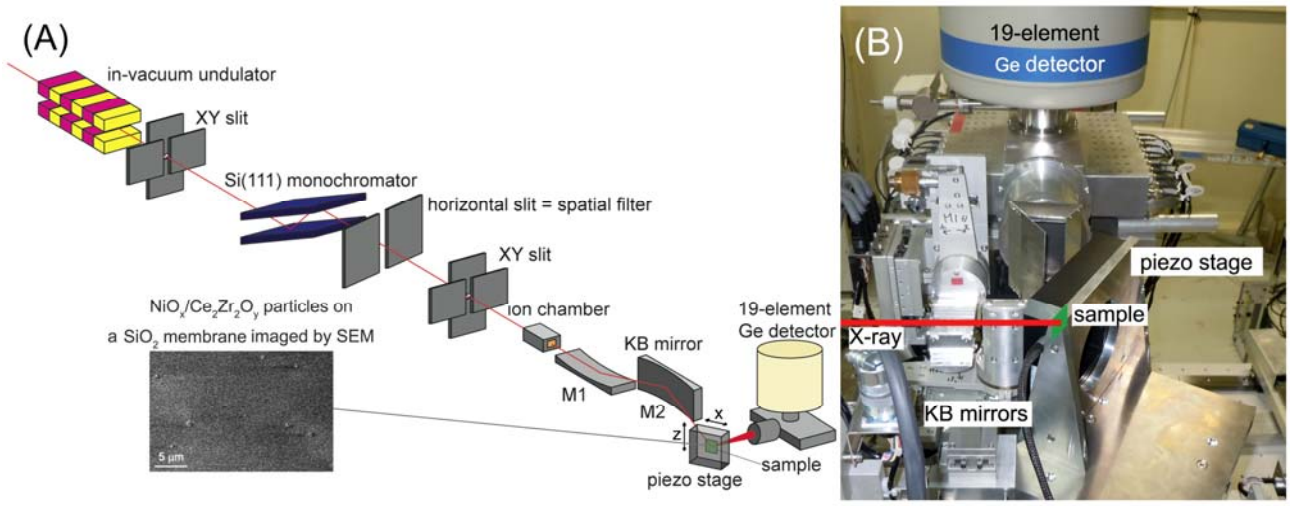

Figure SI 4: (A) A schematic diagram and (B) experimental setup of μ-XAFS.

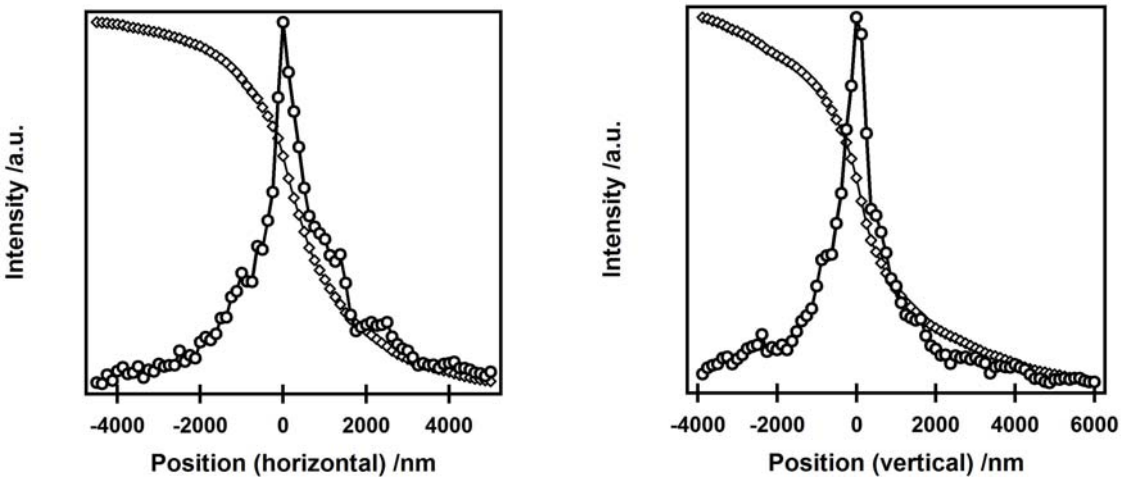

Figure SI 5: Measured profiles of focused beam at the X-ray energy of 8 keV. (left) Beam profile in the horizontal direction and (right) beam profile in the vertical direction. ◇: Raw data of knife-edge scan and ○: numerical derivative of the raw profiles.

2. Conventional XAFS

Conventional XAFS measurements using mm-order X-ray beam were conducted at the BL12C station at KEK-PF (2.5 GeV, 450 mA). X-rays were monochromatized by a Si(111) double-crystal monochromator and X-ray beam size was 1 mm (h) x 1 mm (v). An ion chamber filled with N_2 was used to detect I_0 and that filled with the mixture of N_2 (85%) and Ar (15%) (in a transmission mode) or a Lytle detector filled with Ar (in a fluorescent mode) was used to detect I. XAFS spectra were measured in step-scan mode at room temperature.

3. In-situ μ-XAFS cell

An in-situ XAFS cell was used for scanning μ-XRF and μ-XAFS measurements.

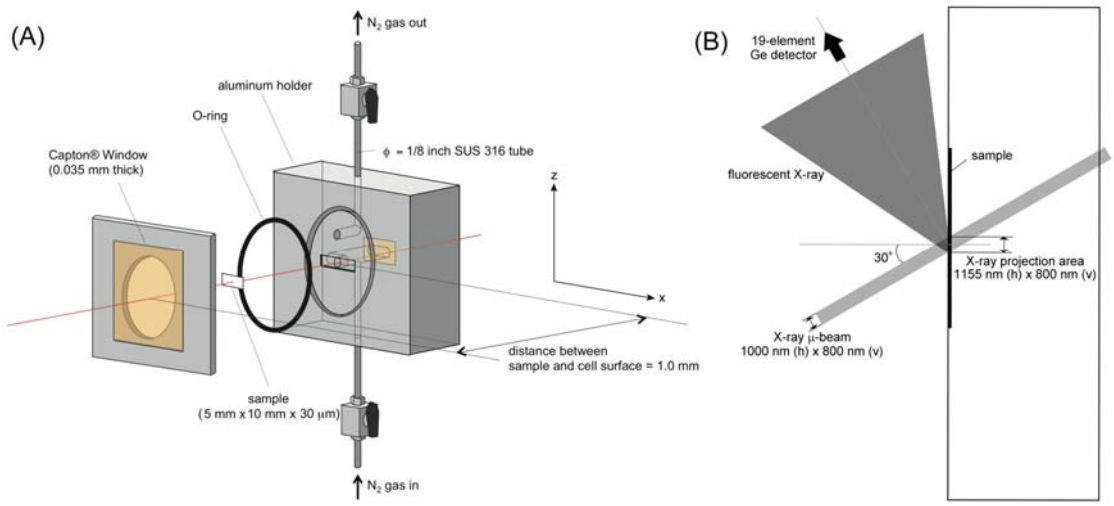

Figure SI 6: (A) A schematic of an in-situ μ-XAFS cell.
(B) A schematic of X-ray projection and the angle of incidence to the sample.

Electronic Supplementary Information 3

Table SI 2: Catalytic performances of methane steam reforming at 923 K over different catalysts

Catalyst	CH_4 conv.%	H_2O conv.%	Selectivity C% (CO/CO_2)	Selectivity H% (H_2)
$Pt/Ce_2Ze_2O_8$	39	49	81 / 19	96
$Pt/Ce_2Ze_2O_7$	39	47	80 / 20	93
$NiO_x/Ce_2Ze_2O_8$	0	0	- / -	-
$NiO_x/Ce_2Ze_2O_7$	75	95	89 / 9	91
$NiO_x/Ce_2Ze_2O_7$[a]	94	>99	98 / 2	96

$CH_4/H_2O/He$ = 2.8/2.8/94.4, catalyst = 0.1 g, GHSV = 14,700 h^{-1}. [a] 973 K.

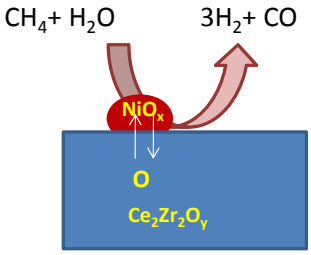

Electronic Supplementary Information 4

1. Background subtraction and extraction of Ni K-edge EXAFS oscillations

EXAFS spectra were analyzed by Ifeffit (Athena and Arthemis) ver. 1.2.11 [7]. Background subtraction was performed with Autobk and Spline smoothing algorithm in the Athena program. k^3-Weighted EXAFS oscillations were Fourier transformed into *R*-space.

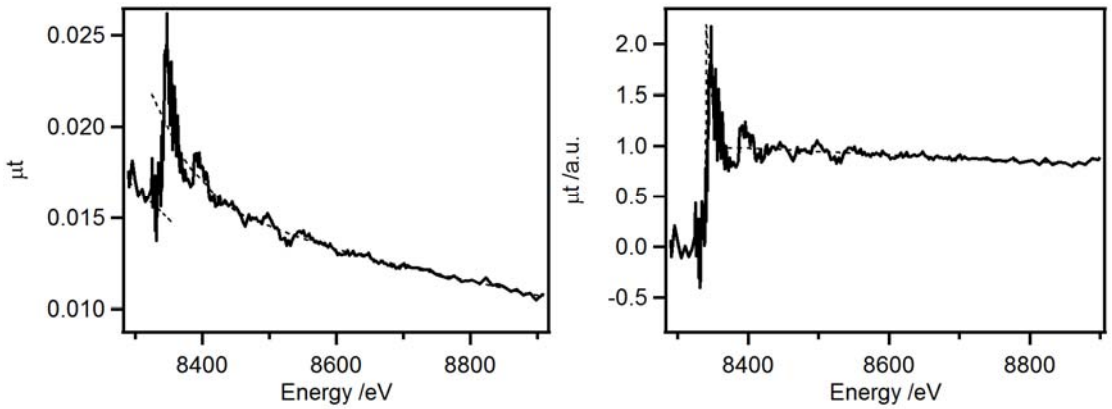

Figure SI 7: (left) A raw spectrum of Ni K-edge μ-XAFS of a $NiO_x/Ce_2Ze_2O_8$ single particle. Bold line: raw data and dashed lines: pre- and post-edge lines for normalization. (right) A normalized μ-XAFS spectrum of the raw μ-XAFS data. Bold line: normalized data and dashed line: background line for the extraction of EXAFS oscillation.

2. Curve-fitting analysis of Ni K-edge EXAFS in *R*-space

Curve-fitting analysis in *R*-space was carried out, considering single scattering of 1st and 2nd coordination shells of Ni oxide. *k*- and *R*-range for the curve-fitting were 30-110 nm^{-1} and 0.1-0.3 nm, respectively. Fitting parameters were coordination number (CN), interatomic distance (*R*), Debye-Waller factor (σ^2), and correction-of-edge energy (ΔE_0). Phase shifts and backscattering amplitudes were calculated by the FEFF8 code [8]. R-factor (R_f) of the curve-fitting in *R*-space was defined as equations (eq. 1),

$$R_f = \frac{\sum_i \left\{ \left[\mathrm{Re}\left(\tilde{\chi}_{\mathrm{data}}(R_i) - \tilde{\chi}_{\mathrm{fit}}(R_i) \right) \right]^2 + \left[\mathrm{Im}\left(\tilde{\chi}_{\mathrm{data}}(R_i) - \tilde{\chi}_{\mathrm{fit}}(R_i) \right) \right]^2 \right\}}{\sum_i \left\{ \left[\mathrm{Re}\left(\tilde{\chi}_{\mathrm{data}}(R_i) \right) \right]^2 + \left[\mathrm{Im}\left(\tilde{\chi}_{\mathrm{data}}(R_i) \right) \right]^2 \right\}} \qquad \text{(eq. 1).}$$

$\tilde{\chi}(R)$s were Fourier transforms of k^3-weighted EXAFS oscillations.

3. Curve-fitting analysis of Ni K-edge EXAFS in *k*-space

Curve-fitting analysis in *k*-space was also carried out, considering multiple scattering taken into account up to 6th coordination, 9 shells with the half path length up to 0.52 nm. *k*-Range for the curve-fitting was 30-110 nm^{-1}. Fitting parameters were S_0^2, isotropic distance expansion/contraction (α), correction-of-edge energy (ΔE_0), and eight Debye-Waller factors (σ^2), for every single scattering path and multiple scattering paths of 4th coordination [9]. Coordination number (CN) and distance (*R*) of the shell were represented as CN = S_0^2 x (degeneration), and *R*= α x (initial half path length (R_{eff})), respectively. The degeneration and R_{eff} of each shell were delivered from model structure given by XRD [10]. Phase shifts and backscattering amplitudes were calculated by the FEFF8 code [8]. R-factor (R_f) of the curve-fitting in *k*-space was defined as equations (eq. 2),

$$R_f = \frac{\sum_i \{ [\tilde{\chi}_{\mathrm{data}}(k_i) - \tilde{\chi}_{\mathrm{fit}}(k_i)]^2 \}}{\sum_i \{ [\tilde{\chi}_{\mathrm{data}}(k_i)]^2 \}} \qquad \text{(eq. 2).}$$

$\tilde{\chi}(k)$s were k^3-weighted EXAFS oscillations.

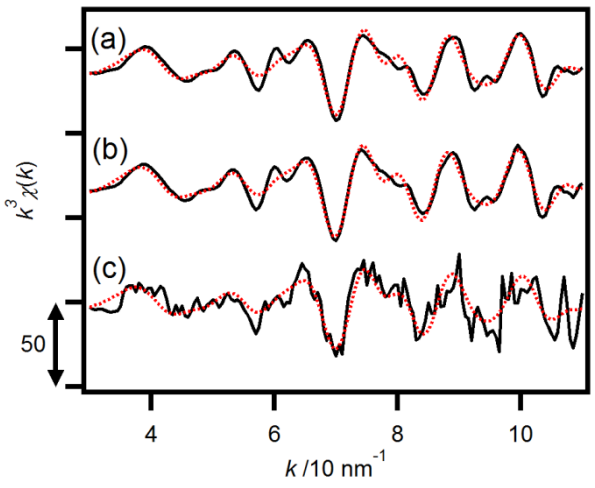

Figure SI 8: k^3-Weighted $\chi(k)$ oscillations of (a) conventional EXAFS of NiO, (b) conventional EXAFS of $NiO_x/Ce_2Zr_2O_8$, and (c) μ-EXAFS of $NiO_x/Ce_2Zr_2O_8$.
Black lines: observed data and red dotted lines: curve-fitted data.

Table SI 3 Results of curve-fitting analysis of Ni K-edge EXAFS in *k*-space

Shell	degen.	R_{eff} /nm	CN	R /nm	σ^2 /10^{-5} nm
NiO measured by conventional EXAFS (beam size: 1 mm x 1 mm)					
k = 30 – 110 nm^{-1}, R_f = 10%, S_0^2 = 0.96 ± 0.11, α = 1.000 ± 0.005, ΔE_0 = -1 ± 3 eV					
Ni(0)-O(1)-Ni(0)	6	2.0842	5.8 ± 0.7	0.208± 0.001	5.6
Ni(0)-Ni(2)-Ni(0)	12	2.9475	11.5 ± 1.3	0.295 ± 0.001	6.4
Ni(0)-O(3)-Ni(0)	8	3.6099	7.7 ± 0.9	0.361 ± 0.002	18 ± 33
Ni(0)-Ni(4)-Ni(0)	6	4.1684	5.8 ± 0.7	0.417± 0.002	-0 ± 10
Ni(0)-Ni(4)-O(1)-Ni(0)	12	4.1684	11.5 ± 1.3	0.417± 0.002	7 ± 2
Ni(0)-O(1)-Ni(4)-O(1)-Ni(0)	6	4.1684	5.8 ± 0.7	0.417± 0.002	2 ± 9
Ni(0)-O(5)-Ni(0)	24	4.6604	23.1 ± 2.6	0.466 ± 0.002	9 ± 12
Ni(0)-O(5)-O(1)-Ni(0)	48	4.8461	46.1± 5.3	0.485 ± 0.002	
Ni(0)-Ni(6)-Ni(0)	24	5.1052	23.1 ± 2.6	0.510 ± 0.002	7 ± 2
$NiO_x/Ce_2Zr_2O_8$ measured by conventional EXAFS (beam size: 1 mm x 1 mm)					
k = 30 – 110 nm^{-1}, R_f = 15%, S_0^2 =1.03 ± 0.09, α = 1.000 ± 0.004, ΔE_0 = -2 ± 2 eV					
Ni(0)-O(1)-Ni(0)	6	2.0842	6.2 ± 0.6	0.208 ± 0.001	5.6
Ni(0)-Ni(2)-Ni(0)	12	2.9475	12.4 ± 1.2	0.295 ± 0.001	6.4
Ni(0)-O(3)-Ni(0)	8	3.6099	8.3 ± 0.8	0.361 ± 0.001	21 ± 35
Ni(0)-Ni(4)-Ni(0)	6	4.1684	6.2 ± 0.6	0.417 ± 0.001	0 ± 7
Ni(0)-Ni(4)-O(1)-Ni(0)	12	4.1684	12.4 ± 1.2	0.417 ± 0.001	7± 1
Ni(0)-O(1)-Ni(4)-O(1)-Ni(0)	6	4.1684	6.2 ± 0.6	0.417 ± 0.001	2 ± 6
Ni(0)-O(5)-Ni(0)	24	4.6604	24.8 ± 2.4	0.466 ± 0.002	9 ± 10
Ni(0)-O(5)-O(1)-Ni(0)	48	4.8461	49.5 ± 4.8	0.485 ± 0.002	
Ni(0)-Ni(6)-Ni(0)	24	5.1052	24.8 ± 2.4	0.511 ± 0.002	7 ± 1
$NiO_x/Ce_2Zr_2O_8$ measured by μ-EXAFS (beam size: 1000 nm x 800 nm)					
k = 30 – 110 nm^{-1}, R_f = 45%, S_0^2 = 0.96 ± 0.19, α = 0.988 ± 0.010, ΔE_0 = -7 ± 6 eV					
Ni(0)-O(1)-Ni(0)	6	2.0842	5.7 ± 1.2	0.206 ± 0.002	5.6
Ni(0)-Ni(2)-Ni(0)	12	2.9475	11.5 ± 2.3	0.291 ± 0.003	6.4
Ni(0)-O(3)-Ni(0)	8	3.6099	7.6 ± 1.5	0.357 ± 0.003	21
Ni(0)-Ni(4)-Ni(0)	6	4.1684	5.7 ± 1.2	0.412± 0.004	8 ± 112
Ni(0)-Ni(4)-O(1)-Ni(0)	12	4.1684	11.5 ± 2.3	0.412± 0.004	9 ± 6
Ni(0)-O(1)-Ni(4)-O(1)-Ni(0)	6	4.1684	5.7 ± 1.2	0.412± 0.004	6 ± 47
Ni(0)-O(5)-Ni(0)	24	4.6604	22.9 ± 4.6	0.460 ± 0.004	13 ± 44
Ni(0)-O(5)-O(1)-Ni(0)	48	4.8461	45.8 ± 9.2	0.479 ± 0.005	
Ni(0)-Ni(6)-Ni(0)	24	5.1052	22.9 ± 4.6	0.504 ± 0.005	8 ± 4

References

[7] B. Ravel and M. Newville, *J. Synchrotron Rad.*, 2005, **12:4,** 537; M. Newville, *J. Synchrotron Rad.*, 2001, **8**, 322.

[8] J. J. Rehr, R.C. Albers, *Rev. Mod. Phys.*, 2000, **72**, 621.

[9] E. Groppo, C. Prestipino, C. Lamberti, P. Luches, C. Gipvanardi, F. Boscherini, *J. Phys. Chem. B*, 2003, **107**, 4597.

[10] R. W. Cairns, E. Ott, *J. Am. Chem. Soc.*, 1933, **55**, 527.